Zn²⁺ induces hyperpolarization by activation of a K⁺ channel and increases intracellular Ca²⁺ and pH in sea urchin spermatozoa

Carmen Beltrán[#a], **Esmeralda Rodríguez-Miranda**[#b], **Gisela Granados-González**[c], **Lucia García de De la Torre**[d], **Takuya Nishigaki**[a], and **Alberto Darszon**[a,*]

[a]Departamento de Genética del Desarrollo y Fisiología Molecular, Instituto de Biotecnología, Universidad Nacional Autónoma de México, Cuernavaca, Morelos CP 62210, México.

[b]Departamento de Medicina y Nutrición, División de Ciencias de la Salud, Universidad de Guanajuato; Campus León. Guanajuato CP 37320, México.

[c]Facultad de Ciencias, Universidad Autónoma del Estado de México, Toluca, Estado de México CP 50000, México.

[d]Departamento de Bioquímica, Centro de Estudios Avanzados (CINVESTAV), México D. F. CP 07360, México.

[#] These authors contributed equally to this work.

Abstract

Zinc (Zn^{2+}) has been recently recognized as a crucial element for male gamete function in many species although its detailed mechanism of action is poorly understood. In sea urchin spermatozoa, Zn^{2+} was reported as an essential trace ion for efficient sperm motility initiation and the acrosome reaction by modulating intracellular pH (pH_i). In this study we found that submicromolar concentrations of free Zn^{2+} change membrane potential (Em) and increase the concentration of intracellular Ca^{2+} ($[Ca^{2+}]i$) and cAMP in *Lytechinus pictus* sperm. Our results indicate that the Zn^{2+} response in sperm of this species mainly involves an Em hyperpolarization caused by K^+ channel activation. The pharmacological profile of the Zn^{2+}-induced hyperpolarization indicates that the cGMP-gated K^+ selective channel (tetraKCNG/CNGK), which is crucial for speract signaling, is likely a main target for Zn^{2+}. Considering that Zn^{2+} also induces $[Ca^{2+}]i$ fluctuations, our observations suggest that Zn^{2+} activates the signaling cascade of speract, except for an increase in cGMP, and facilitates sperm motility initiation upon spawning. These findings provide new insights about the role of Zn^{2+} in male gamete function.

Keywords

Zinc; calcium; membrane potential; potassium channels; cAMP; pH

*Corresponding author: Phone.: +52(777) 329 1650; Fax.: +52(777) 317 2388. darszon@ibt.unam.mx (A. Darszon)..

Introduction

Although Zn^{2+} is a trace element, it is known to be essential for a wide range of biological processes: transcription, cell division, proliferation, immune function, defense against free radicals and fertilization (Pluth et al., 2011). In mammals, it has been known for long time that Zn^{2+} concentration in the seminal fluid is notably high (Hidiroglou and Knipfel, 1984; Mawson and Fischer, 1953). In fact, the highest concentration in the human body is in the seminal plasma (3 mM; (Saaranen et al., 1987)). Zn^{2+} has also been proposed to stabilize chromatin (Bjorndahl and Kvist, 2010) and regulate sperm capacitation (Andrews et al., 1994; Aonuma et al., 1978; Lishko et al., 2010). Furthermore, it was recently reported that Zn^{2+} is also important for male gamete motility regulation in the nematode *C. elegans* (Liu et al., 2013).

Upon dilution of sea urchin sperm in seawater, metal chelators such as EDTA, EGTA, phenantroline and cysteine, at concentrations that do not alter the Ca^{2+} or Mg^{2+} levels (0.1-1 mM), delay motility initiation and inhibit the AR induced by egg jelly (Clapper et al., 1985; Johnson and Epel, 1983). Among the trace ions in seawater (such as Cu^{2+} and Ni^{2+}), only Zn^{2+} can rescue these chelator inhibitory effects, indicating a crucial role of this divalent cation in sea urchin sperm physiology. In addition, Zn^{2+} is able to induce the AR of *Lytechinus pictus* spermatozoa, although its physiological relevance is unknown. The action of Zn^{2+} in sea urchin spermatozoa has been attributed to pH_i regulation (Clapper et al., 1985).

It is well established that echinoderm spermatozoa respond to sperm-activating peptides (SAPs) derived from the egg jelly of the same species which regulate motility (Suzuki, 1995). Speract is the first structurally identified SAP from the egg jelly of *Hemicentrotus pulcherrimus* (Suzuki et al., 1981) and *Strongylocentrotus purpuratus* (Hansbrough and Garbers, 1981), and also stimulates *L. pictus* spermatozoa (Guerrero et al., 2010; Nishigaki and Darszon, 2000). Speract binding to its receptor in the flagella plasma membrane stimulates the synthesis of cGMP (Garbers, 1989) which directly activates the cGMP-gated K^+ selective channel (tetraKCNG/CNGK) inducing a K^+ efflux and a membrane hyperpolarization (Babcock et al., 1992; Bonigk et al., 2009; Galindo et al., 2007). This hyperpolarization leads to increases in pH_i (Lee, 1984), $[Ca^{2+}]i$, and cAMP levels (Beltran et al., 1996). All these changes induced by speract, except for the cGMP increase, are inhibited by elevating the K^+ concentration in seawater (Harumi et al., 1992).

In this study we show that submicromolar free Zn^{2+} concentrations induce similar sperm responses as speract does including Em changes, cAMP elevation and $[Ca^{2+}]_i$ fluctuations except for the cGMP increase in *L. pictus* spermatozoa. We discuss the molecular mechanisms and physiological significance of Zn^{2+} for sea urchin spermatozoa.

Material and Methods

Gametes and reagents

L. pictus sea urchins were obtained from Marinus (Long Beach, CA, USA). Dry sperm were collected after intracelomic injection of 0.5 M KCl and kept on ice until used. The

fluorescent dyes 3,3'-dipropylthiadicarbocyanine iodide (DiSC3(5)), Fluo-4-AM, Quin-2 and 5-(and-6)-Carboxyfluorescein diacetate were obtained from Molecular Probes (Eugene, OR, USA). Anhydrous dimethylsulfoxide (DMSO), tolbutamide, glibenclamide, were from Sigma-Aldrich. $ZnSO_4$ was from Merck. Charybdotoxin and Iberiotoxin were from Alomone Labs. The Kits to measure cAMP (TRK 432) and cGMP (TRK 500) were from Amersham. Speract was synthesized in Professor Possani's Laboratory (IBT-UNAM) and fucose sulfate polymer (FSP) was prepared according to the previous report (Garbers et al., 1983). The rest of the reagents used were of the highest quality available.

Composition of artificial seawater (ASW)

Normal ASW was prepared with the following composition (in mM): 465 NaCl, 26 $MgCl_2$, 10 KCl, 30 $MgSO_4$, 10 $CaCl_2$, 2.5 $NaHCO_3$ and 0.1 EDTA (or otherwise indicated) with pH 8.0 by NaOH. Ca^{2+}-free pH 8.0 (0CaSW) or 1 mM Ca^{2+} pH 7.0 (1CaSW) ASWs were the same except for the indicated $CaCl_2$ concentration and pH. High K^+ ASW (50KSW) contained 50 mM KCl. Cl^--free ASW (0ClSW) was prepared by substituting NaCl and KCl with each metanesulphonate salt and substitution of $MgCl_2$ and $CaCl_2$ with each sulfate salt. In all cases the osmolarity was 950-1000 mOsm.

Fluorescence measurements with sperm suspension

Fluorometric measurements were performed in an OLIS-upgraded SLM 8000 Aminco spectrofluorometer with a temperature-controlled cell holder (14 °C) and a magnetic stirrer. Spermatozoa $[Ca^{2+}]_i$ and pH_i measurements were done according to Rodríguez and Darszon (Rodriguez and Darszon, 2003). Briefly, diluted (1:5) dry sperm in 1CaSW containing 20 μM of Quin-2-AM or Fluo 4-AM without or with 0.5 % Pluronic F-127 or 10 μM Carboxyfluorescein diacetate were incubated for 3 h at 14 °C in the dark. After loading with these fluorescent dyes, 10 ml of 1CaSW were added to the sperm suspension. Coelomocytes and spines were precipitated by mild centrifugation (121 g for 7 min at 4 °C) and the sperm suspension was applied to further centrifugation (1000 g for 8 min at 4 °C) to eliminate the dyes remaining in the media. The sperm pellet was resuspended in the original volume of 1CaSW and kept on ice in the dark until used. A 10 μl aliquot of the loaded sperm was added to a flat-bottom glass tube containing 800 μl ASW. After 30 seconds, an agonist was added using a Hamilton syringe. Fluorescence intensities (excitation/emission wavelength) for Quin-2 (340/490 nm), Fluo-4 (505/525 nm) and Carboxyfluorescein diacetate (490/535 nm) were recorded every 0.5 s.

For Em experiments, 10 μl of diluted (1:10 in 1CaSW) sperm were added to 800 μl of ASW plus 0.7 mM EDTA and 0.5 μM DiSC3(5). The EDTA concentration for Em measurements was increased because DiSC3(5) induces the acrosomal reaction in ASW with 0.1 mM EDTA, but not in 0.8 mM EDTA. Fluorescence intensities of DiSC3(5) (640/670 nm) were registered every 0.5 s. After 2-3 minutes, a protonophore (CCCP 1 μM) was added to avoid mitochondrial membrane potential interference. Once the fluorescence reached the equilibrium, an agonist was added. DiSC3(5) fluorescence was calibrated using 1 μM valinomycin and sequential additions of KCl. Em was calculated according to the Nernst equation assuming that the intracellular K^+ concentration is 180 mM (Babcock et al., 1992). For fluorometric experiments, stock solutions of Fluo-4-AM (1 mM) and

Carboxyfluorescein diacetate (1 mM) and DiSC3(5) (0.8 mM) were made in anhydrous DMSO.

Single cell fluorescence imaging

Fluorescence imaging was carried out as previously reported (Nishigaki et al., 2004). Briefly, Fluo-4-labeled spermatozoa were adhered to glass coverslips coated with 50 Pg/ml poly-L-lysine solution (Sigma) and mounted into a micro incubator, PDMI-2 (Harvard Apparatus, Holliston, MA, USA) maintained at 14 °C. Fluorescence images were acquired using a Nikon DIAPHOT 300 inverted microscope with a Nikon Plan Apo 60X objective lens (1.4 NA) and a custom-built stroboscopic illumination system (Nishigaki et al., 2006) with a Chroma filter set (Ex, HQ470/40x; DC, 505DCXRU; Em, HQ510LP (Chroma Technology)). Images were acquired with a Quantix 57 camera (Photometrics Inc.) under the continuous (stream) acquisition mode.

Determination of cAMP and cGMP levels

Sperm diluted (1:200) in 0CaSW with 1 mM 3-isobutyl-1-methylxanthine (IBMX) were incubated with a ligand (Zn^{2+} or speract) for 1 min at 14 °C. Subsequently, the sperm suspension was transferred to a boiling bath to quench the enzymatic reaction and extract nucleotides. TRK 432 or TRK 500 Kits of Amersham were used to measure cAMP or cGMP concentration, respectively.

Estimation of free Zn^{2+} concentration

The free Zn^{2+} concentration in ASW after various Zn^{2+} additions was estimated using a WinMaxC 2.4 software package (Stanford University, Chris Patton http://www.stanford.edu/~cpatton/downloads.htm). DisC3(5) contains a certain amount of Zn^{2+} as a contaminant and though small amount of DisC3(5) (0.5 PM) should not significantly affect the total Zn^{2+}, in most Em experiments ASW containing 0.8 mM EDTA was used. Addition of 10 μM $ZnSO_4$ to ASW containing 0.8 mM EDTA yields ~ 0.2 nM free Zn^{2+}.

Data normalization

Although the absolute changes in the sperm Em obtained within one season are very reproducible, there is variability between experiments with cells from different seasons. For this reason we normalized the data in order to compare them. Furthermore, in experiments where high K^+ (50KSW) was used to block the speract responses it is difficult to calibrate Em using the Nernst equation. Therefore, Em changes in 50KSW were expressed with F/F_0, where F is fluorescence intensity of DisC3(5) and F_0 is a F value just before addition of Zn^{2+}.

Statistics

Student's t test or one-way ANOVA were used for statistical evaluations. Differences among experimental conditions were considered significant when $p < 0.05$.

Results

Zn^{2+} changes membrane potential (Em) and increases pH_i and $[Ca^{2+}]_i$

It is known in sea urchin sperm that Zn^{2+} increases pH_i (Clapper et al., 1985). Since Zn^{2+} is also known to induce the AR in *L. pictus* spermatozoa, we determined changes of Em, pH_i, and $[Ca^{2+}]_i$ triggered by Zn^{2+} as well as those induced by FSP, the natural AR inducer, and speract. The upper records in Figure 1 show that addition of 10 μM Zn^{2+} (0.2 nM free Zn^{2+}), FSP (~100 nmol fucose/ml) and 100 nM speract causes a transient Em hyperpolarization followed by a depolarization. The Zn^{2+}-induced Em changes are different from those triggered by FSP (middle upper trace), but rather similar to those induced by speract. The three inducers altered pH_i in a somehow similar fashion (center traces). While the $[Ca^{2+}]_i$ increase induced by speract is a transient, those induced by Zn^{2+} and FSP are relatively permanent probably due to the induction of AR (lower records). It is worth noting that the FSP induced $[Ca^{2+}]_i$ changes presented in Fig. 1B were performed using Quin-2 (see Methods) and thus appear smaller than those induced by Zn^{2+} and speract where Fluo-4 was used.

Zn^{2+} hyperpolarizes L. pictus sperm through K^+ channel activation—As a next step, we measured Em changes with different concentrations of Zn^{2+}. Figure 2A shows representative records of Em changes induced by different concentrations of Zn^{2+} and Figure 2B, the average of Em hyperpolarization. Using the results from Figure 2B, we estimated a DL_{50} of Zn^{2+} for the *L. pictus* sea urchin sperm hyperpolarization of 0.38 μM.

A simple mechanism for the Em hyperpolarization might be the activation of electrogenic K^+ efflux or Cl^- influx. Therefore, we explored these two possibilities by altering the ionic compositions of artificial seawater. As shown in Figure 3A, high K^+ ASW (50KSW) effectively inhibited the Em hyperpolarization induced by Zn^{2+}, although the subsequent Em depolarization was not affected significantly. In contrast, Cl^--free ASW (0ClSW) had a small effect on Em hyperpolarization induced by Zn^{2+} (Fig. 3B). These results suggest that one of the principal targets for Zn^{2+} may be a K^+ channel of sea urchin spermatozoa.

Effects of K^+ channel blockers on Zn^{2+}-induced Em hyperpolarization

In order to determine the type of K^+ channel involved in the Zn^{2+}-induced Em changes, we treated the spermatozoa with several K^+ channel blockers. As seen in Figure 4A, 20 mM of TEA (tetraethylammonium), which blocks many types of K^+ channel including one activated by FSP (Guerrero and Darszon, 1989), did not inhibit the Zn^{2+}-induced hyperpolarization. It was reported that Zn^{2+} activates K_{ATP} channels in pancreatic beta cells and brain nerve terminals (Bancila et al., 2005; Bloc et al., 2000; Matias et al., 2010; Prost et al., 2004), but two K_{ATP} channel blockers, either tolbutamide (Fig. 4B) or glibenclamide (Fig. 4C), did not inhibit the Zn^{2+}-induced hyperpolarization. Moreover, neither Charybdotoxin, a blocker of BK/Slo1 (Gimenez-Gallego et al., 1988; Miller et al., 1985) and Kv1 K^+ channels (Grissmer et al., 1994), nor Iberiotoxin another blocker for BK/Slo1 K^+ channel (Galvez et al., 1990) inhibited the Zn^{2+}-induced hyperpolarization (Fig. 4D). Notably, none of these K^+ channel inhibitors were able to significantly decrease the magnitude of the Zn^{2+} induced Em hyperpolarization; instead some reagents rather

enhanced it (Fig. 4E). These results better correspond to the pharmacological profile of tetraKCNG/CNGK, which is key to the speract signaling cascade, reported before (Bonigk et al., 2009; Galindo et al., 2007).

Zn^{2+} induces an increase in cAMP but not in cGMP

Since cyclic nucleotides play fundamental roles in the speract signaling (Darszon et al., 2008; Darszon et al., 2011; Kaupp et al., 2008), we determined the effect of Zn^{2+} on cyclic nucleotides in the cells. Speract elevates the cGMP concentration and this occurs more prominently in high K^+ (50 mM) condition (Fig. 5A), which appears to prevent guanylyl cyclase inactivation (Harumi et al., 1992; Ward et al., 1986). In contrast, Zn^{2+} did not alter the level of cGMP either in normal K^+ (10 mM) or high K^+ condition (Fig. 5A). However, Zn^{2+} was able to induce an increase in the cAMP concentration, as speract does (Fig. 5B and Fig. S1). Furthermore, the increase in cAMP induced by Zn^{2+} was inhibited in high K^+ (Fig. 5B), as in the case of speract. These results suggest that Zn^{2+} activates a K^+ channel, possibly tetraKCNG/CNGK, without altering the cGMP concentration.

Reducing agents partially inhibit the Zn^{2+}-induced hyperpolarization

Previous work implicates cysteine residues as part of the Zn^{2+} binding site that regulates some ionic channels (Choi et al., 2001; Gore et al., 2004; Hou et al., 2010). The role of cysteines in the Zn^{2+}-triggered hyperpolarization was assessed under reducing and non-reducing conditions. DTT is a strong reducing agent that also acts as a metal chelator. As shown in figures 6A&C, 5 mM DTT diminishes (~60%) the Zn^{2+}-triggered hyperpolarization, but does not affect the one induced by Speract (Figs. 6B&C). As DTT is a Zn^{2+} chelator, we tested another cysteine reducing agent such as E-mercaptoethanol that is not considered a Zn^{2+} chelator. This latter reducing agent also inhibited the Zn^{2+}-triggered hyperpolarization but to a lesser extent (~34%) (Fig. 6A&C). These findings suggest that cysteines do participate in this event. It is worth pointing out that the Speract induced hyperpolarization was not significantly sensitive to -mercaptoethanol or DTT. Notably, the depolarization and repolarization that follow the initial hyperpolarization induced by Zn^{2+} was differentially inhibited by DTT (~90%) and β-mercaptoethanol (~70%), while the one triggered by Speract was insensitive to both reducing agents.

Zn^{2+} triggers $[Ca^{2+}]_i$ fluctuations

One of the striking effects of speract on sea urchin sperm is the induction of $[Ca^{2+}]_i$ fluctuations (Wood et al., 2003). Surprisingly, we observed that Zn^{2+} induces $[Ca^{2+}]_i$ fluctuations in a similar way as speract does (Fig. 7). As expected, 50KSW completely blocked the $[Ca^{2+}]_i$ fluctuations induced by Zn^{2+} (Fig. 7) as in the case of speract (Wood et al., 2003). These results support our hypothesis, namely, that Zn^{2+} activates the tetraKCNG/CNGK channel.

High K^+ ASW only partially inhibits Zn^{2+}-induced increases in pHi and $[Ca^{2+}]_i$

It is known that all speract-induced sperm responses, except for the cGMP increase, are suppressed in high K^+ seawater (Harumi et al., 1992). However, we observed that Zn^{2+} only mildly inhibits an Em depolarization under these conditions (Fig. 3A). Therefore, we

explored the effects of Zn^{2+} on $[Ca^{2+}]$ and pH_i changes in the presence of high external K^+. Unexpectedly, although the Zn^{2+} induced increases in pH_i (Fig. 8A&C) and $[Ca^{2+}]_i$ (Fig. 8B&C) were smaller in 50KSW, a significant fraction of them persisted. These results suggest that there may be another target (or targets) for Zn^{2+} besides a K^+ channel in *L. pictus* sperm.

Discussion

The tetraKCNG/CNGK channel as a principal target of Zn^{2+}

It was known that Zn^{2+} is involved in pH_i regulation in sea urchin sperm, but it had not been explored whether this divalent cation affects other physiological parameters such as Em or $[Ca^{2+}]_i$. Therefore, we first determined how Zn^{2+} affects sperm Em, pHi and $[Ca^{2+}]_i$, and compared these responses to those induced by FSP and speract. Remarkably, our results show that Zn^{2+} also triggers sperm Em and Ca^{2+} changes besides alkalinizing pH_i (Fig. 1), as FSP and speract do. Zn^{2+} potently hyperpolarized sperm Em in a dose-dependent manner (Fig. 2). This Zn^{2+}-induced hyperpolarization is likely due to the activation of K^+ channels since 50KSW efficiently inhibited the hyperpolarization, but 0ClSW did not (Fig. 3B). However, none of the K^+ channel blockers so far tested efficiently inhibited the Zn^{2+}-induced hyperpolarization. TEA, a general K^+ channel blocker, did not affect Zn^{2+} induced hyperpolarization. Two K_{ATP} channel blockers, Tolbutamide or Glibenclamide, were unable to inhibit the Zn^{2+}-induced hyperpolarization although K_{ATP} channels are known to be activated by low Zn^{2+} concentrations (Bloc et al., 2000; Prost et al., 2004). Considering the proposed speract signaling cascade of sea urchin sperm, at least two K^+ channels could potentially be responsible for the main component of the Zn^{2+}- induced hyperpolarization; the TetraKCNG (Galindo *et al*., 2007) and a Ca^{2+} dependent K^+ channel (CaKC) (reviewed in Darszon *et al*., 2011). The fact that the Zn^{2+}-triggered hyperpolarization in *L. pictus* sperm was ~30 % reduced in the absence of external Ca^{2+} (Fig. S2) is, in principle, consistent with the participation of CaKCs. However, two peptide blockers of BK/Slo1, Charibdotoxin (also for Kv1 channels) and Iberiotoxin, did not significantly alter the hyperpolarization magnitude. These results may indicate the minor participation of another Ca^{2+} dependent K^+ channel such as the small conductance SK channel (Adelman *et al*., 2012). Aside from this minor component, the pharmacological profile determined here coincides with the one displayed by the cGMP-gated K^+ channel in sea urchin sperm reported by Galindo et al. previously (Galindo *et al*., 2000) and thereafter identified as tetraKCNG/CNGK channel (Bonigk *et al*., 2009; Galindo *et al*., 2007).

If Zn^{2+} directly activates tetraKCNG/CNGK channel, this divalent cation should stimulate the speract signaling cascade. This proposal is further supported by two different lines of experimental evidence. One is that Zn^{2+} increases cAMP levels depending on the extracellular K^+ concentration (Fig. 5B). The other is that Zn^{2+} induces sperm $[Ca^{2+}]_i$ fluctuations as speract does (Fig. 7), in spite of not increasing cGMP levels. These findings altogether are consistent with the proposal that Zn^{2+} activates tetraKCNG/CNGK channels in sea urchin sperm. However, since there is no specific channel blocker for this channel, its heterologous expression will be required to establish if Zn^{2+} directly activates tetraKCNG/CNGK or not.

Cysteine residues have been found as part of the Zn^{2+} binding site that regulates several membrane proteins including ionic channels (Choi *et al*., 2001; Gore *et al*., 2004). Our experiments showed that neither DTT nor -mercaptoethanol, two reducing agents, decreased the hyperpolarization triggered by Speract (Fig. 6B&C), however, both compounds inhibited the Zn^{2+}- induced hyperpolarization (Fig. 6A&C; ~60 % and ~35 %, respectively). It is important to point out that the TetraKCNG contains three extracellular cysteines (C214 in IS5-S6; C1311 in IIIS5-S6 and C1946 in IVS5-S6) one of which could be a Zn^{2+} target. Our findings thus suggest that the K^+ channel activated by Zn^{2+} has a cysteine binding site and if it is tetraKCNG, the Zn^{2+} binding site and the one for speract are independent. Certainly it is possible that a sea urchin sperm K^+ channel still not described could be the main target of Zn^{2+}.

Other targets of Zn^{2+} besides tetraKCNG/CNGK channel

Although the tetraKCNG/CNGK channel is likely to be the principal target of Zn^{2+} in the sea urchin sperm plasma membrane, it is probably not the only one. High $[K^+]_e$ inhibited only ~50 % of the Zn^{2+}-triggered Ca^{2+} increase (Fig. 4C&D) and ~40 % of the pHi alkalinization. This divalent cation could activate directly or indirectly Ca^{2+} channels besides K^+ channels and the sNHE. It is important to stress that the Zn^{2+} induced increase in pHi does not by itself cause a hyperpolarization ((Garcia-Soto *et al*., 1987) and experiments not shown). Furthermore, Zn^{2+} could affect a carbonic anhydrase found in the *S. purpuratus* genome (similar to carbonic anhydrase 8, NCBI Reference Sequence: XP_795365.2). It is therefore clear that Zn^{2+} has multiple targets in sea urchin sperm as it does in many other cell types.

In high K^+ seawater the speract signaling cascade is completely blocked, except for the cGMP elevation (Harumi *et al*., 1992). Namely, both the pH_i and $[Ca^{2+}]_i$ increases induced by speract are completely suppressed in this condition. In contrast, those induced by Zn^{2+} were only significantly reduced (60 and 40 %, respectively), but not eliminated. Actually, this difference may distinguish the action of Zn^{2+} and speract on *L. pictus* spermatozoa where Zn^{2+} is able to trigger a significantly higher % of AR than speract (Fig. S3A) as previously reported (Clapper *et al*., 1985). In this regard we examined if Zn^{2+} triggers the AR through the same mechanism as FSP does.

Interestingly, while Ca^{2+} in seawater is essential for the FSP-induced AR, it is not for the Zn^{2+}-induced AR (Fig. S3B). Furthermore, though Ca^{2+} channel blockers, Ni^{2+} (300 μM) and nifedipine (20 μM) efficiently inhibit the AR induced by FSP, neither treatments inhibited the Zn^{2+}- induced AR (Fig. S3B). Nifulmic acid, a Cl^- channel blocker, only inhibited the AR induced by FSP, but not the AR induced by Zn^{2+} (Fig. S3B). Although 50KSW efficiently inhibited the AR in both cases, the K^+ channels involved in these two events seems different since TEA inhibits FSP-induced AR in *S. purpuratus* sea urchin sperm (Guerrero and Darszon, 1989), in contrast this blocker did not inhibit the Zn^{2+}- induced AR. This pharmacological profile coincides with that of the Zn^{2+}-induced hyperpolarization (Fig. 4). These findings altogether indicate that Zn^{2+} and FSP trigger the AR through different signaling pathways. It is worth pointing out that in *S. purpuratus* spermatozoa, Zn^{2+} does not induce the AR although it causes Em hyperpolarization and

increases in pH_i and $[Ca^{2+}]_i$ (data not shown). The differential ability of Zn^{2+} to induce AR in the two species probably stems from the fact that *L. pictus* sperm have a lower threshold to trigger this reaction.

Physiological role of Zn^{2+} for sea urchin sperm

It is known that Zn^{2+} plays crucial roles for the initiation of sperm motility and the AR in *L. pictus* sea urchins. In both cases, pH_i regulation might be a key point. It is known that sperm motility is suppressed in the testis by low pH_i principally produced by a high partial pressure of CO_2 (Johnson *et al.*, 1983). Upon spawning, spermatozoa are exposed to seawater that has low partial pressure of CO_2 and high pH (around 8.0), which results in the elevation of pH_i.

It was reported that a Na^+/H^+ exchanger (NHE) is also involved in the alkalinization of the pH_i upon sperm motility initiation (Lee *et al.*, 1983). It has been known that sea urchin sperm possess a unique NHE which is regulated by membrane potential (hyperpolarization) (Lee, 1984; Lee and Garbers, 1986). Now, this NHE is thought to be a sea urchin homolog of sperm specific NHE (sNHE), initially identified in mouse (Nomura and Vacquier, 2006; Wang et al., 2003). Compared to other NHEs in somatic cells, this sNHE contains an extra domain composed of 4 trans-membrane segments in the C-terminus (Wang et al., 2003), which is structurally similar to the voltage sensor domain of voltage-gated channels and voltage-regulated phosphatases (Okamura, 2007). Therefore, it is believed that sNHE is regulated by membrane potential using this putative voltage sensor domain. In the speract signaling cascade, Em hyperpolarization caused by K^+ efflux through tetraKCNG/CNGK channel is supposed to activate the sHNE and lead to pH_i alkalinization (Darszon *et al.*, 2008). Results obtained in this study suggest that the same signaling cascade can be activated by Zn^{2+} upon sperm dilution when seawater contains Zn^{2+}. It is known that low pH seawater can suppress sperm motility (Ohtake, 1976), but the sperm flagella still slightly vibrate in this condition. Related to this fact, low pH (6.0) and high K^+ (50 mM) seawater has been employed as a condition to store immotile spermatozoa for long period (Bracho *et al.*, 1997). Taking all information into account, the Em hyperpolarization caused by Zn^{2+}-induced K^+ efflux might be relevant for sperm motility initiation upon spawning in seawater. It is worth mentioning that, in the ascidian *Ciona intestinalis*, an egg-derived single ligand, a sulfated steroid named SAAF, induces both sperm motility initiation and sperm chemotaxis (Yoshida et al., 1993; Yoshida et al., 2002). SAAF is known to hyperpolarize sperm Em through K^+ efflux (Izumi *et al.*, 1999). Furthermore, it was reported, in gill cells of the mollusk *Mytilus galloprovincialis*, that Zn^{2+} activates a NHE and increases pH_i (Kaloyianni *et al.*, 2006; Koutsogiannaki *et al.*, 2006). Since we observed that Zn^{2+} still increases sperm pH_i in high K^+ seawater (Fig. 8), it cannot be ruled out the possibility that this divalent cation directly activates the sNHE.

Conclusions

We demonstrated that submicromolar free Zn^{2+} in seawater can activate a K^+ channel of sea urchin spermatozoa. Pharmacological profiles suggest that the tetraKCNG/CNGK channel, which plays the fundamental role in the early part of the speract signaling cascade, is a

principal target of Zn^{2+}. Therefore, Zn^{2+} can promote sperm motility initiation upon spawning by sharing actions of speract: increases in pH_i, $[Ca^{2+}]_i$ and cAMP. Further detailed studies, particularly heterologous expression of tetraKCNG/CNGK channel, are necessary to define the molecular action of Zn^{2+} in sea urchin spermatozoa.

Supplementary Material

Refer to Web version on PubMed Central for supplementary material.

Acknowledgments

References

Adelman JP, et al. Small-conductance Ca2+-activated K+ channels: form and function. Annu Rev Physiol. 2012; 74:245–69. [PubMed: 21942705]

Andrews JC, et al. Role of zinc during hamster sperm capacitation. Biol Reprod. 1994; 51:1238–47. [PubMed: 7888501]

Aonuma S, et al. The effect of zinc ions on fertilization of mouse ova in vitro. J Reprod Fertil. 1978; 53:179–83. [PubMed: 580440]

Babcock DF, et al. Early persistent activation of sperm K+ channels by the egg peptide speract. Proc Natl Acad Sci U S A. 1992; 89:6001–5. [PubMed: 1631086]

Bancila V, et al. Two SUR1-specific histidine residues mandatory for zinc-induced activation of the rat KATP channel. J Biol Chem. 2005; 280:8793–9. [PubMed: 15613469]

Beltran C, et al. Membrane potential regulates sea urchin sperm adenylylcyclase. Biochemistry. 1996; 35:7591–8. [PubMed: 8652541]

Bjorndahl L, Kvist U. Human sperm chromatin stabilization: a proposed model including zinc bridges. Mol Hum Reprod. 2010; 16:23–9. [PubMed: 19933313]

Bloc A, et al. Zinc-induced changes in ionic currents of clonal rat pancreatic -cells: activation of ATP-sensitive K+ channels. J Physiol. 529 Pt. 2000; 3:723–34.

Bonigk W, et al. An atypical CNG channel activated by a single cGMP molecule controls sperm chemotaxis. Sci Signal. 2009; 2:ra68. [PubMed: 19861689]

Bracho GE, et al. A method for preparation, storage, and activation of large populations of immotile sea urchin sperm. Biochem Biophys Res Commun. 1997; 237:59–62. [PubMed: 9266829]

Clapper DL, et al. Involvement of zinc in the regulation of pHi, motility, and acrosome reactions in sea urchin sperm. J Cell Biol. 1985; 100:1817–24. [PubMed: 3922992]

Choi Y, et al. Three pairs of cysteine residues mediate both redox and zn2+ modulation of the nmda receptor. J Neurosci. 2001; 21:392–400. [PubMed: 11160420]

Darszon A, et al. Sperm-activating peptides in the regulation of ion fluxes, signal transduction and motility. Int J Dev Biol. 2008; 52:595–606. [PubMed: 18649273]

Darszon A, et al. Calcium channels in the development, maturation, and function of spermatozoa. Physiol Rev. 2011; 91:1305–55. [PubMed: 22013213]

Galindo BE, et al. Participation of a K(+) channel modulated directly by cGMP in the speract-induced signaling cascade of strongylocentrotus purpuratus sea urchin sperm. Dev Biol. 2000; 221:285–94. [PubMed: 10790326]

Galindo BE, et al. Sp-tetraKCNG: A novel cyclic nucleotide gated K(+) channel. Biochem Biophys Res Commun. 2007; 354:668–75. [PubMed: 17254550]

Galvez A, et al. Purification and characterization of a unique, potent, peptidyl probe for the high conductance calcium-activated potassium channel from venom of the scorpion Buthus tamulus. J Biol Chem. 1990; 265:11083–90. [PubMed: 1694175]

Garbers DL. Molecular basis of fertilization. Annu Rev Biochem. 1989; 58:719–42. [PubMed: 2549859]

Garbers DL, et al. Elevation of sperm adenosine 3′:5′-monophosphate concentrations by a fucose-sulfate-rich complex associated with eggs: I. Structural characterization. Biol Reprod. 1983; 29:1211–20. [PubMed: 6317072]

Garcia-Soto J, et al. Internal pH can regulate Ca2+ uptake and the acrosome reaction in sea urchin sperm. Dev Biol. 1987; 120:112–20. [PubMed: 3817283]

Gimenez-Gallego G, et al. Purification, sequence, and model structure of charybdotoxin, a potent selective inhibitor of calcium-activated potassium channels. Proc Natl Acad Sci U S A. 1988; 85:3329–33. [PubMed: 2453055]

Gore A, et al. Inhibitory mechanism of store-operated Ca2+ channels by zinc. J Biol Chem. 2004; 279:11106–11. [PubMed: 14715648]

Grissmer S, et al. Pharmacological characterization of five cloned voltage-gated K+ channels, types Kv1.1, 1.2, 1.3, 1.5, and 3.1, stably expressed in mammalian cell lines. Mol Pharmacol. 1994; 45:1227–34. [PubMed: 7517498]

Guerrero A, Darszon A. Evidence for the activation of two different Ca2+ channels during the egg jelly-induced acrosome reaction of sea urchin sperm. J Biol Chem. 1989; 264:19593–9. [PubMed: 2555326]

Guerrero A, et al. Tuning sperm chemotaxis by calcium burst timing. Dev Biol. 2010; 344:52–65. [PubMed: 20435032]

Hansbrough JR, Garbers DL. Speract. Purification and characterization of a peptide associated with eggs that activates spermatozoa. J Biol Chem. 1981; 256:1447–52. [PubMed: 6256397]

Harumi T, et al. Effects os sperm-activating peptide I on Hemicentrotus pulcherrimus spermatozoa in high potassium sea water. Dev. Growth Differ. 1992; 34:163–172.

Hidiroglou M, Knipfel JE. Zinc in mammalian sperm: a review. J Dairy Sci. 1984; 67:1147–56. [PubMed: 6378991]

Hou S, et al. Zn2+ activates large conductance Ca2+-activated K+ channel via an intracellular domain. J Biol Chem. 2010; 285:6434–42. [PubMed: 20037152]

Izumi H, et al. Membrane hyperpolarization by sperm-activating and -attracting factor increases cAMP level and activates sperm motility in the ascidian Ciona intestinalis. Dev Biol. 1999; 213:246–56. [PubMed: 10479445]

Johnson CH, et al. A volatile inhibitor immobilizes sea urchin sperm in semen by depressing the intracellular pH. Dev Biol. 1983; 98:493–501. [PubMed: 6307774]

Johnson CH, Epel D. Heavy metal chelators prolong motility and viability of sea urchin sperm by inhibiting spontaneous acrosome reactions. J Exp Zool. 1983; 226:431–40. [PubMed: 6886666]

Kaloyianni M, et al. The influence of Zn on signaling pathways and attachment of Mytilus galloprovincialis haemocytes to extracellular matrix proteins. Comp Biochem Physiol C Toxicol Pharmacol. 2006; 144:93–100. [PubMed: 16904382]

Kaupp UB, et al. Mechanisms of sperm chemotaxis. Annu Rev Physiol. 2008; 70:93–117. [PubMed: 17988206]

Koutsogiannaki S, et al. Cytotoxic mechanisms of Zn2+ and Cd2+ involve Na+/H+ exchanger (NHE) activation by ROS. Aquat Toxicol. 2006; 78:315–24. [PubMed: 16737744]

Lee HC. A membrane potential-sensitive Na+-H+ exchange system in flagella isolated from sea urchin spermatozoa. J Biol Chem. 1984; 259:15315–9. [PubMed: 6096367]

Lee HC, Garbers DL. Modulation of the voltage-sensitive Na+/H+ exchange in sea urchin spermatozoa through membrane potential changes induced by the egg peptide speract. J Biol Chem. 1986; 261:16026–32. [PubMed: 2430965]

Lee HC, et al. Changes in internal pH associated with initiation of motility and acrosome reaction of sea urchin sperm. Dev Biol. 1983; 95:31–45. [PubMed: 6825930]

Lishko PV, et al. Acid extrusion from human spermatozoa is mediated by flagellar voltage-gated proton channel. Cell. 2010; 140:327–37. [PubMed: 20144758]

Liu Z, et al. The micronutrient element zinc modulates sperm activation through the SPE-8 pathway in Caenorhabditis elegans. Development. 2013; 140:2103–7. [PubMed: 23578924]

Matias CM, et al. Blockade of presynaptic K ATP channels reduces the zinc-mediated posttetanic depression at hippocampal mossy fiber synapses. Brain Res. 2010; 1320:22–7. [PubMed: 20097182]

Mawson CA, Fischer MI. Zinc and carbonic anhydrase in human semen. Biochem J. 1953; 55:696–700. [PubMed: 13115357]

Miller C, et al. Charybdotoxin, a protein inhibitor of single Ca2+-activated K+ channels from mammalian skeletal muscle. Nature. 1985; 313:316–8. [PubMed: 2578618]

Nishigaki T, Darszon A. Real-time measurements of the interactions between fluorescent speract and its sperm receptor. Dev Biol. 2000; 223:17–26. [PubMed: 10864457]

Nishigaki T, et al. Stroboscopic illumination using light-emitting diodes reduces phototoxicity in fluorescence cell imaging. Biotechniques. 2006; 41:191–7. [PubMed: 16925021]

Nishigaki T, et al. A sea urchin egg jelly peptide induces a cGMP-mediated decrease in sperm intracellular Ca(2+) before its increase. Dev Biol. 2004; 272:376–88. [PubMed: 15282155]

Nomura M, Vacquier VD. Proteins associated with soluble adenylyl cyclase in sea urchin sperm flagella. Cell Motil Cytoskeleton. 2006; 63:582–90. [PubMed: 16847896]

Ohtake H. Respiratory behaviour of sea-urchin spermatozoa. I. Effect of pH and egg water on the respiratory rate. J Exp Zool. 1976; 198:303–11. [PubMed: 12246]

Okamura Y. Biodiversity of voltage sensor domain proteins. Pflugers Arch. 2007; 454:361–71. [PubMed: 17347852]

Pluth MD, et al. Biochemistry of mobile zinc and nitric oxide revealed by fluorescent sensors. Annu Rev Biochem. 2011; 80:333–55. [PubMed: 21675918]

Prost AL, et al. Zinc is both an intracellular and extracellular regulator of KATP channel function. J Physiol. 2004; 559:157–67. [PubMed: 15218066]

Rodriguez E, Darszon A. Intracellular sodium changes during the speract response and the acrosome reaction in sea urchin sperm. J Physiol. 2003; 546:89–100. [PubMed: 12509481]

Saaranen M, et al. Lead, magnesium, selenium and zinc in human seminal fluid: comparison with semen parameters and fertility. Hum Reprod. 1987; 2:475–9. [PubMed: 3667903]

Suzuki N. Structure, function and biosynthesis of sperm-activating peptides and fucose sulfate glycoconjugate in the extracellular coat of sea urchin eggs. Zoolog Sci. 1995; 12:13–27. [PubMed: 7795487]

Suzuki N, et al. Purification and the primary structure of sperm-activity peptides from the jelly coat of sea urchin eggs. Biochem Biophys Res Commun. 1981; 99:1238–44. [PubMed: 7196229]

Wang D, et al. A new sperm-specific Na+/H+ exchanger required for sperm motility and fertility. Nat Cell Biol. 2003; 5:1117–22. [PubMed: 14634667]

Ward GE, et al. Phosphorylation of membrane-bound guanylate cyclase of sea urchin spermatozoa. J Cell Biol. 1986; 103:95–101. [PubMed: 2873144]

Wood CD, et al. Speract induces calcium oscillations in the sperm tail. J Cell Biol. 2003; 161:89–101. [PubMed: 12695500]

Yoshida M, et al. Sperm chemotaxis during the process of fertilization in the ascidians Ciona savignyi and Ciona intestinalis. Dev Biol. 1993; 157:497–506. [PubMed: 8500656]

Yoshida M, et al. A chemoattractant for ascidian spermatozoa is a sulfated steroid. Proc Natl Acad Sci U S A. 2002; 99:14831–6. [PubMed: 12411583]

Zn^{2+} hyperpolarizes sea urchin sperm membrane potential.

The cGMP-gated K^+ channel seems to be a main target of Zn^{2+}.

Zn^{2+} induces $[Ca^{2+}]_i$ fluctuations.
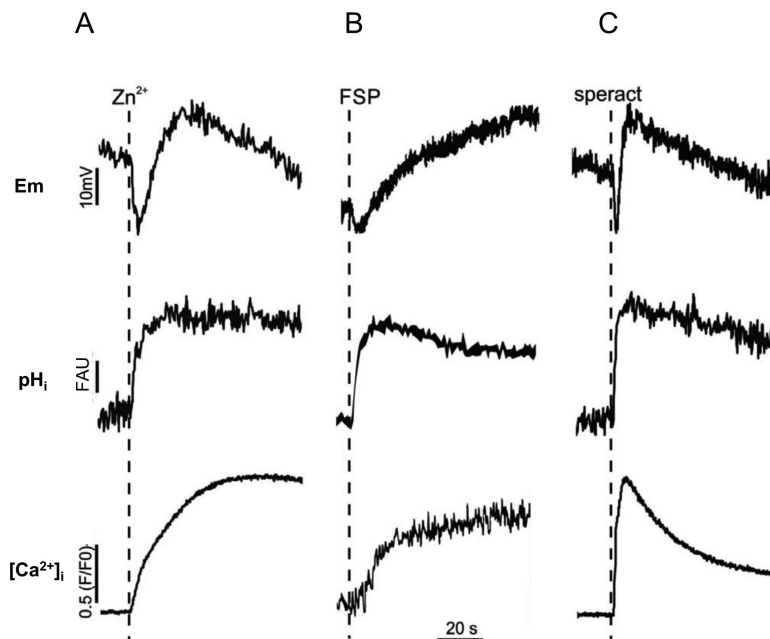
Zn^{2+} increases cAMP, but not cGMP.

Fig. 1.
Zn^{2+} changes Em and increases pH_i and $[Ca^{2+}]_i$ as FSP and Speract.

Em (upper row records), pH*i* (middle row records) and $[Ca^{2+}]_i$ (lower row records) of sea urchin sperm were measured in cell populations as described in methods. Dotted lines indicate a point of agonist addition: A, Zn^{2+} (10 M total); B, FSP (~100 nmol fucose/ml); C, 100 nM Speract. The free concentration of Zn^{2+} was estimated to be 0.2 nM in Em measurement (0.8 mM EDTA) and 1.8 nM in pH_i and $[Ca^{2+}]_i$ measurements (0.1 mM EDTA). Downward and upward deflections of each parameter indicate hyperpolarization and depolarization of Em and decreases and increases of $[Ca^{2+}]_i$ and pH_i, respectively. The scale of each parameter Em (mV), pH_i (FAU, Fluorescence Arbitrary Units) and $[Ca^{2+}]_i$ ((F/F0); where F is Fluo-4 (or Quin-2) fluorescence intensity and F0 is the fluorescence before adding speract or Zn^{2+}) is indicated with vertical bars. The time scale was indicated by horizontal bars. Records shown in this figure are representative of at least three different animals. Zn^{2+} and FSP induced similar amounts of acrosome reaction that were 57%.
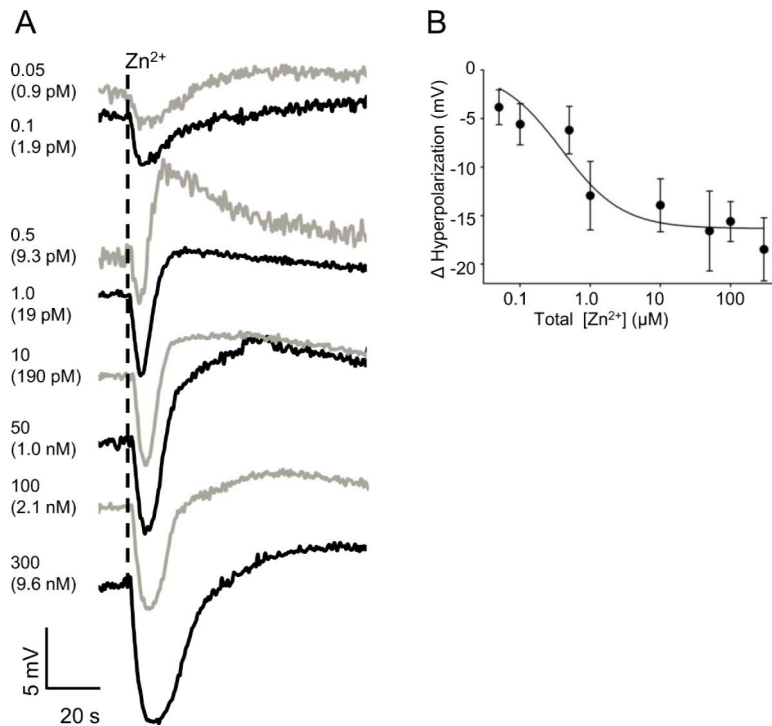
Fig. 2.
Zn^{2+} hyperpolarizes the sperm Em in a dose dependent manner.

Representative traces of the sperm Em changes triggered by different Zn^{2+} concentrations (0.05-300 μM) are shown in panel A. Each number indicates the total concentration of Zn^{2+} in PM and the estimated free Zn^{2+} concentration is in parenthesis. To avoid trace confusion, black and gray lines were used alternatively. Panel B shows the best fit curve of the hyperpolarization change as a function of log[Zn^{2+}] for three different animals with triplicate measurements. One way ANOVA was used to examine if the differences between different Zn^{2+} concentrations was significant at *p < 0.05.
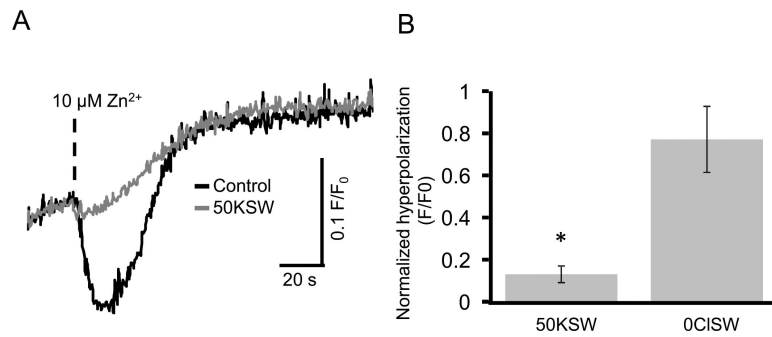
Fig. 3.

High K^+ ASW (50KSW) inhibits the Zn^{2+}-induced hyperpolarization.

Panel A shows representative sperm Em responses to 10 μM Zn^{2+} (0.2 nM free Zn^{2+}) in normal ASW (black line) and in 50KSW (gray line). Panel B shows the magnitude of Em hyperpolarization (mean ± SE) induced by 10 μM Zn^{2+} in 50KSW and Cl^- free ASW (0ClSW). The magnitude of hyperpolarization (delta F/F_0) was normalized against control experiments performed in normal ASW. Statistically significant differences are indicated by asterisks (n = 5 for 50KSW and n = 4 for 0ClSW; *p 0.05).
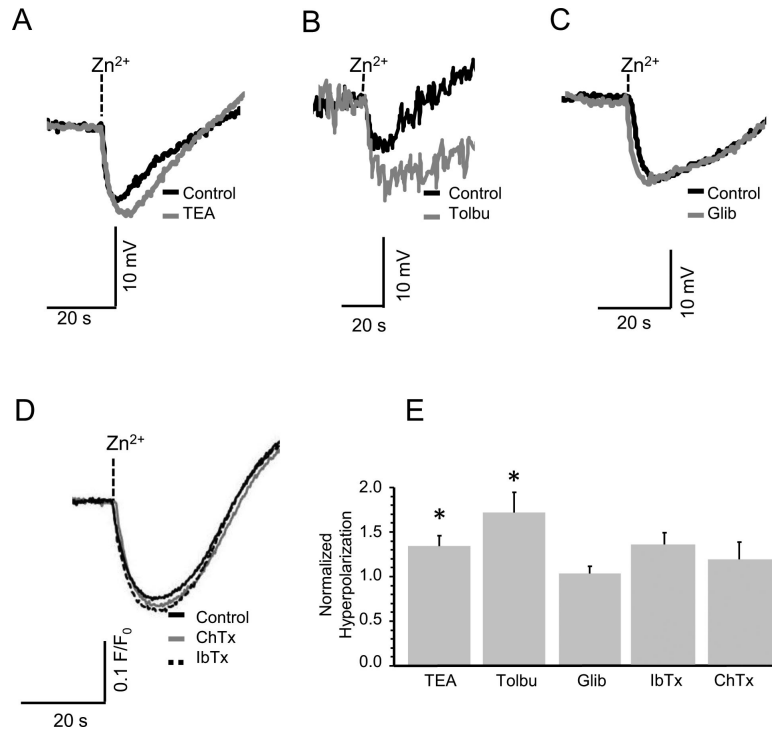
Fig. 4.

The Zn^{2+}-triggered hyperpolarization is not inhibited by several K^+ channel blockers. Traces A-D indicate representative Em changes induced by 10 μM Zn^{2+} (0.2 nM free Zn^{2+}) in ASW containing 20 mM tetraethylammonium (TEA) in panel A, 300 μM Tolbutamide (Tolbu) in panel B, 20 μM Glibenclamide (Glib) in panel C, or 100 nM Charybdotoxin (ChTx) or 100 nM Iberiotoxin (IbTx) in panel D. Black traces are in the absence of blockers (control) and gray traces are in the presence of each K^+ blocker. In panel D, broken trace indicates in the presence of IbTx. Panel E shows the mean ± SE of the normalized hyperpolarization change of sperm from three different animals with triplicate measurements. Asterisks (*) indicate statistically significant differences compared to controls using Student's t test (n= 3; p 0.05). We also analyzed the data with ANOVA comparing each condition, however no significant differences between groups were found.
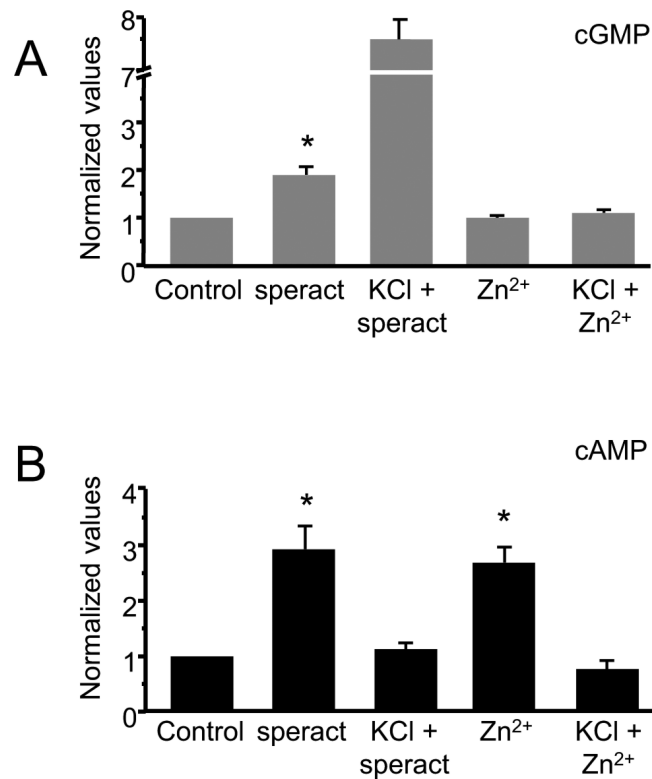
Fig. 5.

Zn^{2+} and speract raise cAMP levels but only speract increases cGMP.

Concentration of cGMP (panel A) and cAMP (panel B) in spermatozoa diluted in 0CaSW with 1 mM IBMX were measured in the presence or absence of 100 nM Speract or 10 μM Zn^{2+} (0.07 nM free Zn^{2+}). Also, the same measurements were performed in high K^+ (50 mM) condition. The mean ± SE of three experiments with sperm from different animals with triplicate measurements were normalized against the control (the resting level of cyclic nucleotides). Asterisks (*) indicate statistically significant differences compared to controls ($p < 0.05$).
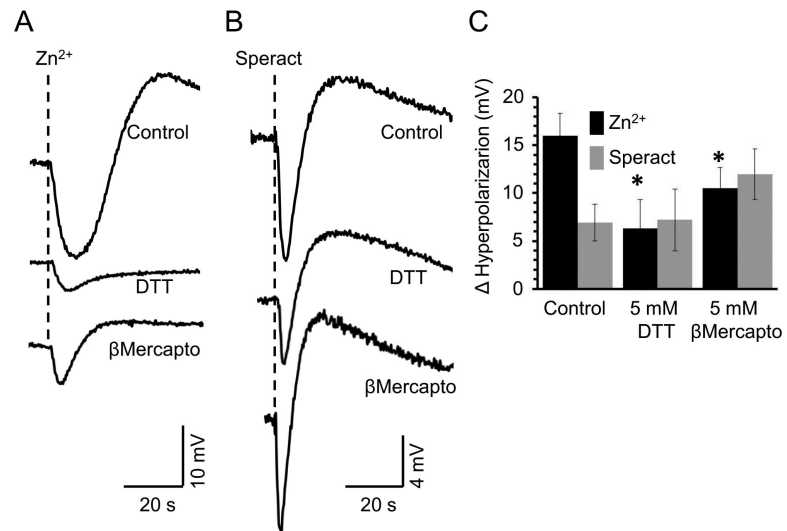
Fig. 6.
The Zn^{2+}-triggered hyperpolarization is inhibited by DTT and β-mercaptoethanol , two reducing agents. Sperm diluted in ASW containing or not (Control) 5 mM of DTT or β-mercaptoethanol, were exposed to either 10 μM Zn^{2+} (A) or 100 nM Speract (B). The mean ± SE of the hyperpolarization change (mV) is shown (n 5; *p 0.05).

Fig. 7.
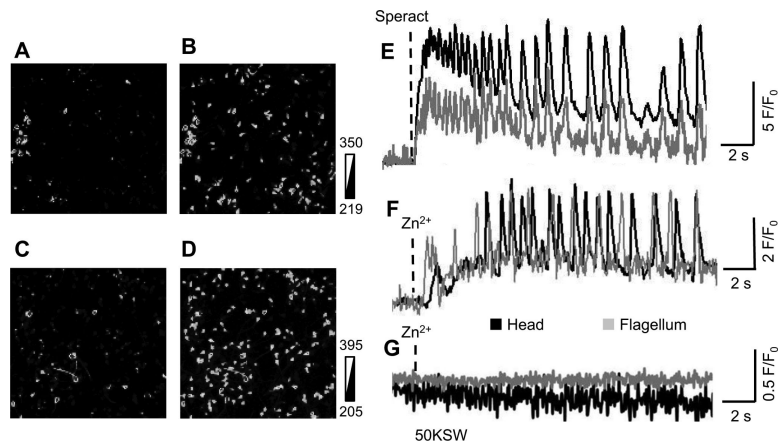Speract and Zn^{2+} induce $[Ca^{2+}]_i$ oscillations in sea urchin sperm.

Ca^{2+} images of individual spermatozoa were acquired using Fluo-4 as described in materials and methods. Panel A and B show representative fluorescence images before (A) and 3 s after addition of 100 nM speract (B). Panel C and D show representative fluorescence images before (C) and 2.5 s after addition of 10 μM Zn^{2+} (total) (D). Fluorescence images (A-D) are expressed as gray scales. Panel E, F and G indicate fluorescence changes (F/F_0) of single spermatozoon (black lines are from the head and gray ones are from the tail). Spermatozoa were stimulated by 100 nM speract (E), 10 μM Zn^{2+} (F) and 10 μM Zn^{2+} in high K^+ ASW, 50KSW (G). The results are representative of 5 independent experiments.
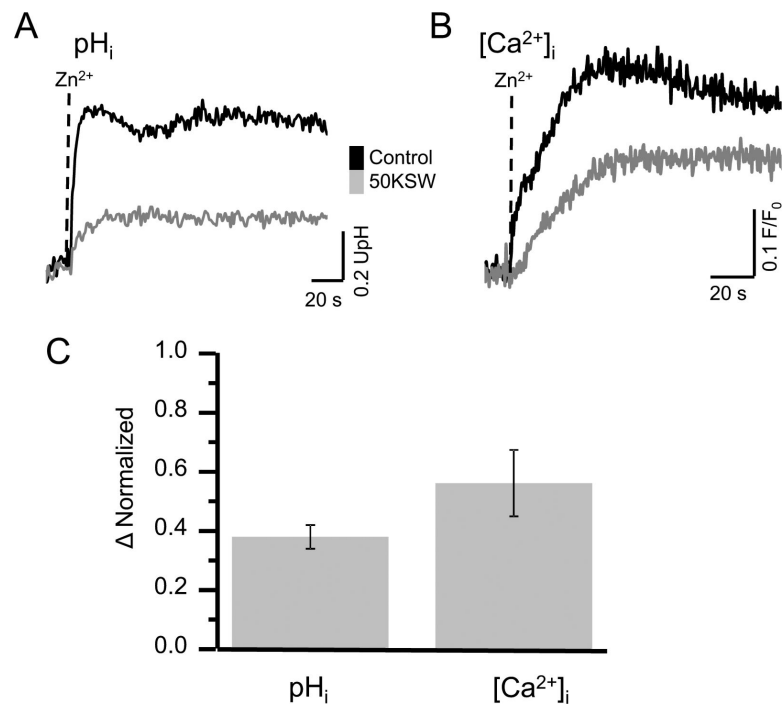
Fig. 8.
High K^+ ASW (50KSW) partially inhibits the Zn^{2+} induced increase in pH_i and $[Ca^{2+}]_i$. Sperm pH_i and $[Ca^{2+}]$ changes induced by 10 µM Zn (1.8 nM free Zn^{2+}) were measured in normal ASW (black line) and 50KSW (gray line) by fluorometry as in Figure 1. Panel A and B show representative traces of pH_i and $[Ca^{2+}]_I$ measurements, respectively. Panel C summarizes the inhibition of the pH_i and $[Ca^{2+}]_i$ increases induced by Zn^{2+} in 50KSW normalized against the values obtained in normal ASW (mean ± SE, n=3 for $[Ca^{2+}]_i$ and n=4 for pH_i).